Virtual Coupling Potential for elastic scattering of ^{10,11}Be on proton and carbon targets

V. Lapoux [a,1,2], N. Alamanos [a], F. Auger [a], Y. Blumenfeld [b], J-M. Casandjian [c], M. Chartier [c,3], M.D Cortina-Gil [c,4], V. Fékou-Youmbi [a], A. Gillibert [a], M. Mac Cormick [c,5], F. Maréchal [b,6], F. Marie [a], W. Mittig [c], F. de Oliveira Santos [c], N. A. Orr [d], A.N. Ostrowski [c,7], S. Ottini-Hustache [a], P. Roussel-Chomaz [c], J-A. Scarpaci [b], J-L. Sida [a,8], T. Suomijärvi [b], J. S. Winfield [c,9]

[a] *CEA-Saclay, DSM/DAPNIA/SPhN, F-91191 Gif-sur-Yvette, France*
[b] *IPN-Orsay, IN2P3-CNRS, F-91406 Orsay, France*
[c] *GANIL, Bld. Henri Becquerel, BP 5027, F-14021 Caen Cedex, France*
[d] *LPC-ISMRA, Bld du Maréchal Juin, F-14050, Caen, France*

Abstract

The ^{10,11}Be(p,p) and (^{12}C, ^{12}C) reactions were analyzed to determine the influence of the weak binding energies of exotic nuclei on their interaction potential. The elastic cross sections were measured at GANIL in inverse kinematics using radioactive ^{10,11}Be beams produced at energies of 39.1 A and 38.4A MeV. The elastic proton scattering data were analyzed within the framework of the microscopic Jeukenne-Lejeune-Mahaux (JLM) nucleon-nucleus potential. The angular distributions are found to be best reproduced by reducing the real part of the microscopic optical potential, as a consequence of the coupling to the continuum. These effects modify deeply the elastic potential. Including the Virtual Coupling Potential (VCP), we show the ability of the general optical potentials to reproduce the data for scattering of unstable nuclei, using realistic densities. Finally, the concepts needed to develop a more general and microscopic approach of the VCP are discussed.

Key words: ^{10,11}Be(p,p), (^{12}C,^{12}C), virtual coupling potential, weakly-bound nuclei
PACS: 24.10.-i, 25.60.-t, 25.60.Bx, 25.40.Cm

[1] Corresponding author
[2] E-mail: vlapoux@cea.fr
[3] present address: Univ. of Liverpool , UK.
[4] present address: Dpto de Particulas, Facultad de Fisica, Santiago de Compostela 15706 Spain.
[5] present address: IPN Orsay, F-91406 Orsay France.
[6] present address : IPHC IReS, BP 28, F-67037 Strasbourg, France.
[7] present address : Institut fr Kernchemie, Universität Mainz, Mainz, Germany.
[8] Present address: CEA DIF/DPTA/SPN, B.P. 12, F-91680 Bruyères-le-Châtel, France.
[9] present address : GSI, Planckstr. 1. 64291 Darmstadt, Germany.

Light neutron-rich exotic nuclei are characterized by weak binding energies. They may develop peculiar structures like neutron-skin or halo structures. For instance, ^{6}He and ^{11}Be develop two-neutron and one-neutron halo, respectively. Another important effect is the couplings to the continuum states. The probability to be excited to continuum states is higher, compared to the stable isotopes, and this may induce new features in the interaction potential. The coupling to the other reaction processes may also be stronger. In principle, to calculate the interaction potential for elastic scattering, one

should include all possible virtual couplings between the ground and higher excited states. These processes remove flux from the elastic channel. This effect is negligible for most stable nuclei, but becomes significant for weakly-bound nuclei [1]. The interaction term arising from couplings to inelastic channels is called the dynamical polarization potential (DPP) [1]. This term is complex, non-local and energy-dependent, it includes the coupling to excited states, the coupling to continuum states or to other reaction processes, like transfer reactions or break-up. We find it more appropriate to rename it as "virtual coupling potential" (VCP). The general formalism for such coupling processes in the interaction potential is described in Feshbach's theory [2]. But its exact calculation would require the precise knowledge of the spectroscopy of the nucleus and the transition strengths to bound and continuum excited states. Due to the difficulty to evaluate these interaction couplings, they are not taken into account *a priori* in the usual optical model approaches. However, in the case of a weakly-bound nucleus like ^{6}Li ($S_{alpha+d}$ = 1.46 MeV) easily described as a two-body nucleus, it was possible to describe microscopically the continuum states and to deduce the effect due to the coupling potential [3] in the elastic scattering of ^{6}Li on various targets. It was shown [1,3] that the coupling effects were responsible for the reduction of the real part of the potential needed to reproduce the elastic data in the framework of the folding model [4].

For exotic isotopes with lower particle thresholds, the coupling between the ground state and the continuum is expected to increase. Our aim is to investigate the effect of the weak binding of exotic nuclei on the elastic scattering data to test the validity of the effective nucleon-nucleon NN interactions used for the reaction analysis, and to know whether the weak binding of exotic nuclei should appreciably enhance the VCP. Finally we want to determine a general form of this potential. In [5], the ^{6}He(p,p) elastic scattering data at 38.3 A.MeV were analyzed using the microscopic JLM potential [6]. It was shown [5] that the angular distributions of ^{6}He on proton are better reproduced with a reduction of the real part of the microscopic optical potential rather than with an enhancement of the imaginary part. The wide angular range of the angular distributions (up to 71.5° c.m.) allowed us to draw this conclusion. This effect was attributed to the continuum couplings. A phenomenological VCP was simulated. The same effect was found in the elastic scattering ^{6}He+^{12}C [7]. The enhancement and the role of the continuum couplings in the case of the weakly-bound radioactive nucleus ^{6}He on proton target have been emphasized in [8] and the polarization potential was deduced microscopically from the inversion of the S-matrix in the framework of the Coupled Discretized Continuum Channels (CDCC) calculations.

Elastic data are well reproduced when the coupling effect is taken into account, as done, for instance, within the CDCC calculations, including some cluster structure or introducing a phenomenological VCP. Through the analysis of such data we can understand how the cross sections are affected by the coupling effects and it is possible to deduce the optical potentials required to describe the direct reactions; afterwards, we can check the validity of the microscopic densities tested in the reaction analysis. A similar analysis was carried out for the neutron-deficient ^{10,11}C [9]. In the case of the elastic scattering ^{8}He+p [10], we found that it was necessary to take into account the coupling to the (p,d) reaction within the coupled-reaction framework. It was shown that the important modification of the potential needed to reproduce the elastic scattering was due to the loss of flux in the one-neutron transfer reaction. In this case, the VCP was mainly produced by the (p,d) coupling effect.

A set of elastic data of light nuclei on protons, including ^{10,11}Be, was presented and analyzed in Ref. [11]. The data were well reproduced using global or microscopic proton-nucleus potentials provided that the real part was reduced or the imaginary part enhanced. However, the data did not extend to large enough angles to choose between the two possibilities.

This article presents new elastic scattering data of ^{10,11}Be on proton and carbon targets, collected at the GANIL (Grand Accélérateur National d'Ions Lourds, Caen, France). The angular distributions were measured at energies close to 40A MeV up to 70° in the center of mass (c.m.) frame for proton scattering, and up to $20^\circ_{c.m}$ for scattering on carbon. The data were collected on a wide angular domain to investigate the VCP effect. The article explains the analysis carried out to discuss the coupling effects induced by ^{10,11}Be.

We first present our measurement. The analysis of the proton-nucleus elastic data is discussed, the VCP is introduced, and its effect is shown on the p-nucleus data. The data for ^{10,11}Be on carbon target are then compared to the folding model calculations

and the influence of the VCP is explained. In conclusion, we discuss the general framework needed to develop a microscopic analysis of the VCP.

The experiment was carried out at the GANIL coupled cyclotron facility. The ^{10,11}Be secondary beams were produced by fragmentation of a 75 MeV/nucleon primary ^{18}O beam on a carbon production target located between the two superconducting solenoids of the SISSI device [12]. The secondary beams were purified with an achromatic degrader set in the beam analysis spectrometer. The ^{10,11}Be beams were obtained at energies of 39.1A and 38.4A MeV, with intensities of the order 10^5 pps and 3.10^4 pps, respectively. They were scattered from a 10 mg/cm^2 thick polypropylene target (density of 0.896 g/cm^3). Elastic angular-dependent cross sections of ^{10,11}Be projectiles on protons and carbon nuclei were measured with the SPEG spectrometer [13]. The scattered particles were identified at the focal plane by the energy loss measured in an ionisation chamber and the residual energy measured in a thick plastic scintillator. The momentum and the angle after the target were obtained by track reconstruction of the trajectories determined by two drift chambers straddling the focal plane of the spectrometer. Position and angle of the projectiles on the target were determined event by event by two beam detectors. The experimental set-up is similar to the one described in [5,7] for the case of ^{6}He on protons and ^{12}C. With the polypropylene reaction target containing both hydrogen and carbon nuclei, we obtained a simultaneous measurement of the cross sections on protons and ^{12}C. The laboratory angle range covered was from 1.3° to 8.5°. The good energy resolution of the SPEG spectrometer ($\frac{\Delta E}{E} = 10^{-3}$) allowed us to extract the elastic scattering data on ^{12}C without any contamination from scattering to the ^{12}C excited states. Cross sections on ^{12}C are dominated at small angles by Coulomb deflection, so the calculation at these angles is not sensitive to the nuclear potential. Consequently, for this angular range, all calculations lead to the same first maximum in the angular distribution, thus providing an absolute normalization for the data on ^{12}C, and as a result on the protons. ^{12}C and ^{10}Be have a first excited state (2^+) at 4.44 and 3.37 MeV, respectively. With the good energy resolution of the SPEG, it was possible to separate elastic scattering of ^{10}Be on carbon from inelastic contributions. This is not the case for ^{11}Be for which the energy of the first excited state $1/2^-$ is at 320 keV, very close to the $1/2^+$ ground state.

With the ECIS code [14], we did coupled-channel calculations to estimate the relative yields of the elastic cross sections versus inelastic ones to the $1/2^-$ for ^{11}Be on p and ^{12}C targets. Phenomenological potentials were employed, and also the known large value for B(E1, $1/2^+_{gs} \rightarrow 1/2^-$)(=0.116 e^2.fm^2 [15,16]). This analysis showed that the inelastic cross sections are at least two orders of magnitude lower than the corresponding elastic cross sections in the angular domain of interest and can be neglected. Higher excitation energy states in ^{11}Be are not bound against neutron emission (S_n = 504 keV) and cannot contribute in the ^{11}Be yield detected in the focal plane of the spectrometer. The data for the elastic scattering of ^{10,11}Be on protons are presented in Figs. 1-2. The angular resolution is of the order of 0.5° in the laboratory system giving errors in the c.m. system of ^{10}Be+p and ^{11}Be+p of 5.5° and 6°, respectively. For ^{10}Be+^{12}C (^{11}Be) , the angular resolution is $0.95^\circ_{c.m.}$ ($1^\circ_{c.m.}$). In the figures, the error bars are statistical and the angular bins correspond to the resolution.

The idea in this article was to examine the validity or limitation of the existing well-established models for the nuclear potential, when we deal with weakly-bound nuclei. In this case, we have to take care about effects which occur at the nuclear surface. It means that coupling effects must be incorporated, whatever the choice made on the NN potential for the folding procedure. Here, we have chosen the effective JLM potential for p+Be and the folding potential for Be+^{12}C with the effective NN interaction CDM3Y6, and from the arguments developed below the potentials of our analysis are fully consistent.

We first want to examine the validity of the microscopic nucleus-nucleon potential for the description of the proton elastic scattering on exotic nuclei. The nucleus-nucleon elastic scattering can be described with the complex nucleon-nucleon interaction JLM [6] deduced from calculations in infinite symmetric nuclear matter with the local density approximation, and for energies up to 160 MeV.
This model generates a complex microscopic potential which only depends on the scattering energy and on the density of the involved nucleus. The potential is written : $U_{JLM} = \lambda_V V + i\lambda_W W$, with λ_V, λ_W the normalization factors of the real V and imaginary W parts of the potential. In the case of stable nuclei, it reproduces successfully a large range of proton and neutron elastic scattering angular dis-

tributions, without any free parameter [17]. In the case of light exotic nuclei, data are well reproduced, provided the imaginary potential be somewhat adjusted by a normalization factor $\lambda_W \sim 0.8$ [18].

The elastic JLM potentials for ^{10,11}Be+p are calculated using the Hartree-Fock (HF) densities described in Ref. [19]. We consider these densities as realistic ones, since the HF calculations were constrained so as to reproduce the neutron separation energies and the matter root mean square (rms) values of these densities are found consistent with the empirical matter rms values deduced from reaction cross sections data. The rms radii of the nuclear proton, neutron, matter, distributions for ^{10,11}Be are r_m=2.44 [r_p = 2.26, r_n= 2.56] fm and 2.92 fm [r_p = 2.27, r_n= 3.24], respectively. In the c.m. angular range from 20° to 40°, there is a large discrepancy between the standard JLM curve (λ_V=1 and λ_W=0.8) and the data.

To improve the agreement with the data, we tried two approaches, either the reduction of the real part, searching for the best $\lambda_V < 1$ value (and keeping $\lambda_W = 0.8$) or the enhancement of the absorption with the increase of the imaginary potential $\lambda_W > 1$ (keeping $\lambda_V = 1$). The curves obtained with these prescriptions are displayed in Figs. 1-2. With this procedure, the best agreement with the ^{10}Be data in the angular domain between 20 and 40° is obtained when λ_V=0.9, (with fixed $\lambda_W = 0.8$) or with λ_W=1.2, (fixed $\lambda_V = 1$). For ^{11}Be, the values of the normalization factors are λ_V=0.75 (fixed $\lambda_W = 0.8$) and $\lambda_W = 1.4$ (fixed $\lambda_V = 1$). As found for ^{6}He [5] the angular distributions for ^{11}Be are better reproduced on the whole angular range when the real part of the JLM potential is scaled down. The origin of this effect can be attributed to the VCP. In Ref. [5], the ^{6}He + p scattering data were reproduced using a phenomenological VCP. Such a potential is a repulsive surface potential, which can produce, in the surface region of the nucleus+target system, a similar effect as the reduction of the real part of the potential. This leads to the global decrease of the cross sections in the angular region from 20 to $40^\circ_{c.m.}$, consistent with the data. Similarly, to reproduce the ^{11}Be + p data, we could use such a phenomenological VCP but, as can be seen in Fig.2, the simple reduction of the real potential is enough to simulate the effects of the VCP for ^{11}Be. This may be attributed to the fact that ^{11}Be displays similar features, as the ones of ^{6}He : a low S_n and the main coupling effects are the coupling to low-lying unbound and continuum states. In contrast, for ^{10}Be, the neutron threshold S_n is higher, at 6.8122 MeV and the main coupling effect could possibly be found in the one-neutron transfer (p,d) or even in the (p,t) reaction. Consequently, a good description of the ^{10}Be+p data would require to go beyond our simple VCP modeling and to investigate carefully the influence of the coupled reaction channels on the elastic scattering. This will be the subject of a further work. For the elastic scattering on the ^{12}C target, the ratio of cross sections in the c.m. frame over the Rutherford cross sections are plotted in Figs. 3-4. The binning of the data corresponds to the angular resolution in the c.m. frame. We carry out the same analysis as done successfully in the case of the ^{6}He+^{12}C data [7]. For this system, it was possible to explain the coupling effects induced by the halo-nucleus ^{6}He using the folding model and a phenomenological VCP in the coupled channel framework.

The cross sections are calculated using the ECIS97 code [14]. The real potentials U_F of ^{10}Be+^{12}C and ^{11}Be+^{12}C are calculated within the framework of the folding model: the potential is obtained by double-folding over the nuclear matter densities of the projectile and target nuclei with the density-dependent NN interaction CDM3Y6 (Paris-form) [20]. The nuclear density of ^{12}C is a 2-parameter Fermi function with radius R = 2.1545 fm, diffuseness a = 0.425 fm, r_m = 2.298 fm [21] which is consistent with the experimentally known charge density. In a first step, we only use the real folding potential and a phenomenological imaginary potential W, which is a Woods-Saxon function parametrized as in Ref. [22] with depth W_I, reduced radius r_I (r_I=$R_I/(A_P^{1/3} + A_T^{1/3})$, A_P and A_T the mass numbers of projectile and target), and diffuseness a_I. These parameters are given in Tab. 1. With the interaction potential defined as $U_F + iW$, the data are not reproduced as shown in Figs. 3-4. As in [5,7], we introduce a phenomenological VCP which is a complex repulsive surface potential simulating the coupling effects. U_{VCP} is complex with the real part $\mathcal{V}_{VCP}$ (and similarly imaginary one $\mathcal{W}_{VCP}$) written as :

$$\mathcal{V}_{VCP} = -4 * V_{vcp} \frac{x_r}{[1+x_r]^2} \quad (1)$$

with $x_r = \exp\left(\frac{r-R_{vcp}}{a_{vcp}}\right)$. We have $V_{vcp} \leq 0$ which gives a repulsive potential. For simplicity, the VCP is written with no radius (R_{vcp} = 0 fm). The total interaction potential is now defined as $U_F + iW +$

U_{VCP} and we adjust the parameters of U_{VCP} in order to reproduce the data. The best agreement obtained is presented with the solid lines in Figs. 3-4. The parameters of U_{VCP} are given in Table 1. This analysis is only a simple model, built in order to exhibit the coupling effects and to propose a simple shape of VCP. A more sophisticated analysis could be undertaken using the coupled reaction framework to explore its origin.

Several theories were developed to have a deeper understanding of the continuum effects : for high-energy reaction studies (few 100A MeV) the role of the continuum coupling has been addressed in several few-body approaches, by implicitly including the coupling to all orders [23–25]. In the study of reaction mechanisms at lower energy (few 10A MeV), the coupling effects have been taken into account by explicitly coupling to a discretized continuum [3,26]. More generally, for the analysis of the one nucleon-transfer reactions and elastic scattering on light targets like deuteron targets, a coupled-reaction framework [27] is needed. A complete study of the ^{10,11}Be scattering would require a precise treatment of the VCP through an explicit calculation of the coupling, as done for instance with the CDCC methods [10]. We should take into account not only the coupling to the one-neutron (p,d) reaction but also to the inelastic scattering. Such work will benefit from the last developments of the nuclear reaction models including the core excitation [28].

In conclusion, our analysis is a first approach to deduce the main features of the VCP for ^{10,11}Be. The elastic scattering of exotic nuclei ^{10,11}Be was calculated using the optical model and a microscopic approach for the proton-nucleus potential, and for the nucleus-^{12}C real potential. Densities taking into account the large extension of these neutron-rich nuclei were included. We found that the elastic scattering data of the exotic nucleus ^{11}Be on a proton is well described with a simple reduction of the real part of the JLM potential. This reduction is able to simulate the coupling effects induced by the weakly-bound projectile. For the analysis of the elastic scattering on carbon target, the coupling effect was introduced explicitly through the parameterization of a VCP.
More generally, to reach an accurate and improved description of the direct reactions with radioactive nuclei, we will have to calculate explicitly the VCP by including the couplings to the excited states, the continuum states and to reaction channels like (p,d) reaction.

Acknowledgments

We thank Dr H. Sagawa, for the ^{10,11}Be density distributions, and Dr. Dao T. Khoa for his folding code, DFPD2. The assistance of the SPEG crew, P. Gangnant and J.-F. Libin, in the preparation and running of the experiment is gratefully acknowledged.

References

[1] M. E. Brandan and G. R. Satchler, Phys. Rep. **285**, 143 (1997).
[2] H. Feshbach, Ann. Phys. **5**, 357 (1958).
[3] Y. Sakuragi, Phys. Rev **C 35**, 2161 (1987).
[4] G.R. Satchler and W.G. Love, Phys. Rep. **55**, 183 (1979).
[5] V. Lapoux et al., Phys. Lett. B **517**, 18 (2001).
[6] J.P. Jeukenne, A. Lejeune and C. Mahaux, Phys. Rev. C **16**, 80 (1977).
[7] V. Lapoux *et al.*, Phys. Rev. C **66**, 034608 (2002).
[8] R.S. Mackintosh and K. Rusek, Phys. Rev. C **67**, 034607 (2003).
[9] C. Jouanne *et al.*, Phys. Rev. C **72**, 014308 (2005).
[10] F. Skaza *et al.*, Phys.Lett. B **619**, 82 (2005).
[11] M. D. Cortina-Gil *et al.*, Phys. Lett. B **401**, 9 (1997).
[12] A. Joubert *et al.*, Particle Accelerator Conference IEEE, Vol.1, 1991, 594.
[13] L.Bianchi *et al.*, Nucl. Instrum. Methods Phys. Res. A **276**, 509 (1989).
[14] J. Raynal, Phys. Rev. C **23**, 2571 (1981); ECIS97 code, priv. co.
[15] D.J Millener, J.W Oness, E.K Warburton, and S.S Hanna, Phys. Rev. C **28**, 497 (1983).
[16] T. Nakamura *et al.*, Phys. Lett. B **394**, 11 (1997).
[17] S. Mellema, R.Finlay, F. Dietrich and F. Petrovich, Phys. Rev. **C 28**, 2267 (1983).
[18] J.S. Petler *et al.*, Phys. Rev. C **32**, 673 (1985).
[19] H. Sagawa, Phys. Lett. B **286**, 7 (1992).
[20] D. Khoa, G.R. Satchler, and W. von Oertzen, Phys. Rev. **C 56** (1997) 954.
[21] M. El-Azab Farid and G.R. Satchler, Nucl. Phys **A438**, 525 (1985).
[22] R. A. Broglia and A. Winther, *Heavy Ions Reactions, Lectures notes*, the Benjamin/Cummings Publishing Company, Inc., 1981.
[23] R. Crespo and R.C. Johnson, Phys. Rev. C **60**, 034007 (1999).
[24] J.S. Al-Khalili and J.A. Tostevin, Phys. Rev. C **57**, 1846 (1998).
[25] R.C. Johnson, J.S. Al-Khalili and J.A.Tostevin, Phys. Rev. Lett. **79**, 2771 (1997).
[26] M. Kamimura *et al.*, Prog. Theor. Phys. Suppl. **89**, 1-118 (1986); N. Austern, Y. Iseri, M. Kamimura, M. Kawai, G. Rawitscher, M. Yahiro, Phys. Rep. **154**, 125 (1987).
[27] N. Keeley, N. Alamanos, and V. Lapoux, Phys. Rev. C **69**, 064604 (2004).

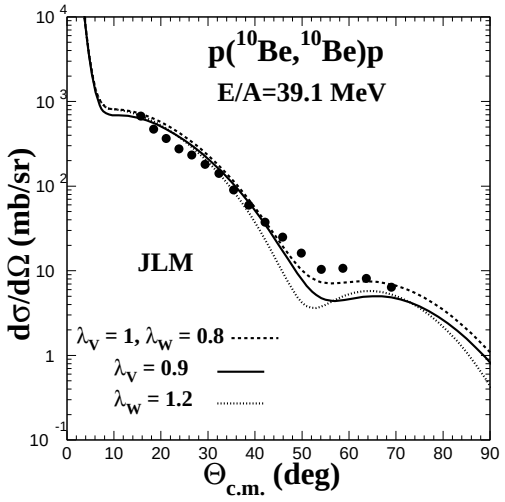

Fig. 1. Cross sections for the ^{10}Be + p elastic scattering at 39.1A MeV compared to calculations using the JLM potential and the "Sagawa" density. The full circles correspond to the data. The dashed line corresponds to the standard JLM calculation for light nuclei. Full line (respectively dotted line) corresponds to calculations in which the real part (imaginary) was renormalized.

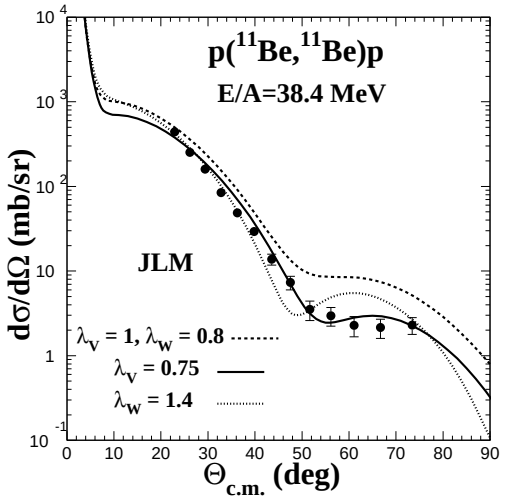

Fig. 2. Same as in Fig. 1 for the ^{11}Be + p elastic scattering at 38.4A MeV.

[28] N.C. Summers, F.M. Nunes and I.J. Thompson, Phys Rev C **73**, 031603 (2006).

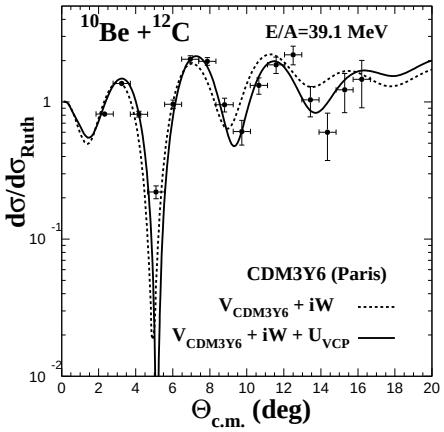

Fig. 3. Cross sections for the ^{10}Be + ^{12}C elastic scattering at 39.1A MeV are compared with calculations using the CDM3Y6 folding potential and the imaginary potential W (dashed line). Data are better reproduced taking into account a complex VCP U_{VCP} (solid line), given in the text.

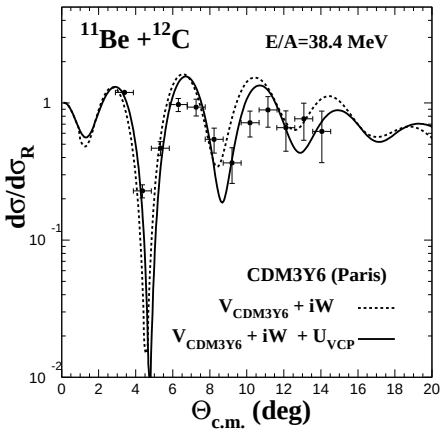

Fig. 4. Same as in Fig. 3 for ^{11}Be at 38.4A MeV.

	W_I (MeV)	r_I (fm)	a_I (fm)	V_{vcp} (MeV)	W_{vcp} (MeV)	a_{vcp} (fm)
^{10}Be	20.9	1.1	0.63	-21.7	-3.8	1.6
^{11}Be	22.5	1.105	0.63	-22.	-5	1.68

Table 1
Parameters of the imaginary part W of the optical potential and of the VCP for ^{10,11}Be on carbon target.